Materials Chemistry and Physics 112 (2008) 1021–1023

Contents lists available at ScienceDirect

Materials Chemistry and Physics

journal homepage: www.elsevier.com/locate/matchemphys

Ferromagnetism and exchange bias in Fe-doped ZnO nanocrystals

Huilian Liu[a,b,c], Jinghai Yang[a,b,c,*], Yongjun Zhang[a], Yaxin Wang[a], Maobin Wei[a]

[a] Physics College of Jilin Normal University, Jilin Province 136000, People's Republic of China
[b] Key Laboratory of Excited State Processes, Changchun Institute of Optics, Fine Mechanics and Physics, Chinese Academy of Sciences, Changchun 130033, People's Republic of China
[c] Graduate School of the Chinese Academy of Sciences, Beijing 100049, People's Republic of China

ARTICLE INFO

Article history:
Received 16 April 2008
Received in revised form 17 June 2008
Accepted 1 July 2008

Keywords:
Diluted magnetic semiconductors
Ferromagnetic
Exchange bias

ABSTRACT

$Zn_{1-x}Fe_xO$ ($x = 0.03, 0.05, 0.08, 0.1$) nanocrystals were synthesized from Zn nitrate and Fe nitrate reduced by citrate. The X-ray diffraction (XRD) shows that $Zn_{1-x}Fe_xO$ ($x \leq 0.08$) samples are single phase with the ZnO-like wurtzite structure, while the secondary phase $ZnFe_2O_4$ is observed in $Zn_{0.9}Fe_{0.1}O$ sample. Magnetic measurements indicate that $Zn_{1-x}Fe_xO$ ($x = 0.03, 0.05, 0.08$) are ferromagnetic at room temperature and appear exchange bias varies with Fe concentration. The origin of the ferromagnetic is given by exchange and Zn vacancies in samples.

1. Introduction

Diluted magnetic semiconductors (DMSs) have been extensively studied for spintronic devices that allow the control of both the spin and charge of carriers [1,2]. For realizing practical spintronic devices, it is essential that the DMS systems display ferromagnetism at room temperature. In the quest for materials with a high transition temperature, transition metal (TM)-doped ZnO has emerged as an attractive candidate based on both theoretical [3] and experimental [4] studies. It is known that the doping of transition metal in ZnO leads to new interesting properties [5,6].

Recently, more and more reports of Fe-doped ZnO diluted magnetic semiconductor prepared by different methods were issued [7–11]. While Shim et al. reported the ferromagnetic behaviors for the Fe-doped ZnO:Cu [12]. Potzger et al. also obtained room temperature ferromagnetism by implanting Fe ions in hydrothermal ZnO single crystals [13]. Wang reported the ferromagnetic behaviors for Fe-doped ZnO bulk samples [14]. However, there are a lot of controversies about whether the observed ferromagnetism is an intrinsic or extrinsic property of the material.

Here, we chose the nanostructure Fe-doped ZnO as study object. Since a clear understanding of finite-size effects on the magnetic mechanism of such systems is essential for the development of high-density magnetic storage media with nanosized constituent particles or crystallites [15]. We report doping Fe into ZnO with varying Fe concentration by decomposing citrate technique, achieve room temperature ferromagnetism (RTFM) and exchange bias in $Zn_{1-x}Fe_xO$ ($x = 0.03, 0.05, 0.08$). The origin of the ferromagnetism in $Zn_{1-x}Fe_xO$ ($x \leq 0.08$) was discussed.

2. Experimental

Zn nitrate [$Zn(NO_3)_2{\cdot}6H_2O$] and appropriate amounts of Fe nitrate [$Fe(NO_3)_3{\cdot}9H_2O$] were dissolved into citric acid [$C_6H_8O_7$] while stiring. The solution was dried at 80 °C to obtain xerogel. After the swelled xerogel was completed at 130 °C, a reticular substance was obtained, then grinded to powders in agate mortar. Sintering the powders was carried out at 600 °C for 10 h under air atmosphere. This method allows mixing of the chemicals at atomic level thus reducing the possibility of undetectable impurity phase. The reaction mechanism of decomposing citrate technique was described previously [16].

Structural characterization of $Zn_{1-x}Fe_xO$ were performed by X-ray diffraction (XRD) on D/max-2500 copper rotating-anode X-ray diffractometer with Cu Kα radiation (40 kV, 200 mA), The size distribution and interplanar distance were investigated by transmission electron microscope (TEM) (200 keV, JEM-2100HR, Japan). Magnetic hysteresis loops of $Zn_{1-x}Fe_xO$ ($x \leq 0.08$) and M–T curve of $Zn_{0.92}Fe_{0.08}O$ were measured by a Lake Shore 7407 vibrating sample magnetometer (VSM). The $Zn_{0.92}Fe_{0.08}O$ was determined by X-ray photoelectron spectroscopy (XPS) (VG ESCALAB Mark II).

3. Results and discussion

Fig. 1 shows the XRD patterns for $Zn_{1-x}Fe_xO$ ($x = 0.03, 0.05, 0.08, 0.1$). Pure wurtzite single phase of ZnO can be obtained below $x = 0.08$ within the sensitivity of XRD. The $Zn_{0.9}Fe_{0.1}O$ shows a coexistence region of the dominant hexagonal phase $Zn_{1-x}Fe_xO$ and a minor spinel phase $ZnFe_2O_4$. With the increase of Fe content ($x \leq 0.08$), the X-ray peak widths increase, suggesting a decrease

* Corresponding author at: Physics College of Jilin Normal University, Jilin Province 136000, People's Republic of China. Tel.: +86 434 3294566; fax: +86 434 3294566.
E-mail address: jhyang1@jlnu.edu.cn (J. Yang).

0254-0584/$ – see front matter.
doi:10.1016/j.matchemphys.2008.07.004

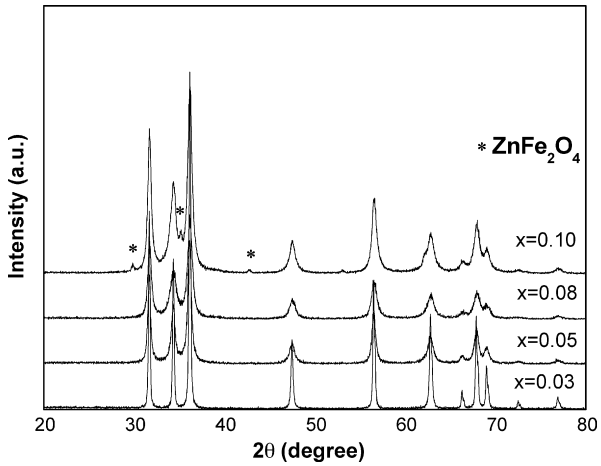

Fig. 1. XRD patterns of the $Zn_{1-x}Fe_xO$ ($x = 0.03, 0.05, 0.08, 0.1$).

in crystalline correlation. The mean particle sizes of the samples ($Zn_{0.92}Fe_{0.08}O$) were also estimated to be around 20 nm using the Scherrer formula.

Fig. 2(a) and (b) shows the results of TEM characterization. Fig. 2(a) shows a low-resolution TEM micrograph for $Zn_{0.92}Fe_{0.08}O$; micrograph reveals the average size of the particles about 20 nm which is consistent with the results of XRD. We concluded that the $Zn_{1-x}Fe_xO$ prepared by decomposing citrate technique are nanostructured materials. High-resolution TEM micrographs are presented in Fig. 2(b), which shows that the interplanar distance of fringes is 0.26 nm which is corresponding to the (0 0 2) planes of wurtzite ZnO.

All the nanoparticles in the sample are single crystalline and free from any major lattice distortion. With the results of XRD and HRTEM images, we believe that the Fe ions substitutionally incorporated into the crystal lattice of ZnO.

Magnetic measurements on $Zn_{1-x}Fe_xO$ ($x = 0.03, 0.05, 0.08$) were performed at room temperature using vibrating sample magnetometer. Fig. 3(a) shows the magnetization versus magnetic field (M–H) loops. All the samples show clear RTFM and with the Fe concentration increases, the saturated magnetic moment per Fe of $Zn_{1-x}Fe_xO$ ($x \leq 0.08$) decreases. The $Zn_{1-x}Fe_xO$ ($x = 0.03$, 0.05, 0.08) samples individual possess moment of 0.17 μ_B per Fe atom, 0.13 μ_B per Fe atom, and 0.065 μ_B per Fe atom, which are much less than the theoretically calculated value. The moment of per magnetic cation can be less due to several factors [15]. Firstly, the weaker exchange between particles in nanostructured material can lower the magnetic moment, which is due to the nanostructured nature of the material. Secondly, with the concentration of Fe is very close to the cationic percolation threshold, nearest-neighbor antiferromagnetic interaction (superexchange) between the Fe ions can lower the magnetic moment. Thirdly, the presence of any small randomly distributed cluster undetected by XRD can also be the cause for the same. The consistent drop in moment per Fe atom of with the concentration of Fe increase could be an increasing occurrence of antiferromagnetic coupling between Fe pairs occurring at shorter separation distances. The inset of Fig. 3(a) shows temperature dependence of magnetic moment for $Zn_{0.92}Fe_{0.08}O$ under 1 KOe. With increasing temperature, the magnetization moment for $Zn_{0.92}Fe_{0.08}O$ decreased and reached to a Curie temperature (T_C) below 340 K, which excluded the possible existence of the metallic iron or iron oxides. Because the Curie temperature (T_C) of them are higher than 340 K, and an increase in Fe concentration would presumably increase magnetization signature if they were responsible for the ferromagnetic behavior, which opposited to the experimental result. We concluded that the ferromagnetism of the $Zn_{1-x}Fe_xO$ in this study is an intrinsic property of Fe-doped ZnO.

Fig. 3(b) is local enlarged patterns for Fig. 3(a) from it we can see clearly that these loops show obvious asymmetric about zero fields. This may be exchange bias varies with Fe concentration. In order to provide strong evidence, a series of M–H curves for $Zn_{1-x}Fe_xO$ ($x = 0.08$) sample are taken at various temperature under 1500 Oe. The temperature dependence of coercive field (H_C) is plotted in inset of Fig. 3(b). We can see that H_C increase clearly with the decrease of T which is opposite to the Fe-doped ZnO bulk samples [14] and corresponds to the characteristics of the exchange bias. However, the previous reports suggest the exchange bias was observed only when the ferromagnetic semiconductors were capped by the additional antiferromagnetic layers [17,18]. Further research might need to be done to clarify what caused exchange bias.

On addressing the origin of FM in the Fe-doped ZnO nanoparticles, the $Zn_{0.92}Fe_{0.08}O$ was determined by XPS. Fig. 4 shows typical XPS spectra of $Zn_{0.92}Fe_{0.08}O$. The peaks at 710.3 and 723.3 eV were corrected with the C1s reference (284.6 eV), which is corresponding to the binding energy of Fe $2p_{3/2}$ and Fe $2p_{1/2}$. They can be Gaussian fitted with Fe^{2+} (fixing $2p_{3/2}$ peak at 710.3 eV and $2p_{1/2}$ peak at 722.3 eV) and Fe^{3+} (fixing $2p_{3/2}$ peak at 710.7 eV and $2p_{1/2}$ peak at 724.0 eV) [19] components. Usually, if Fe is present in the substitutional site in a defect-free ZnO crystal, the valence state of Fe will be +2. However, the XPS result confirms the presence of uncoupled Fe^{3+} within the sample. In Ref. [20], the associated secondary phase

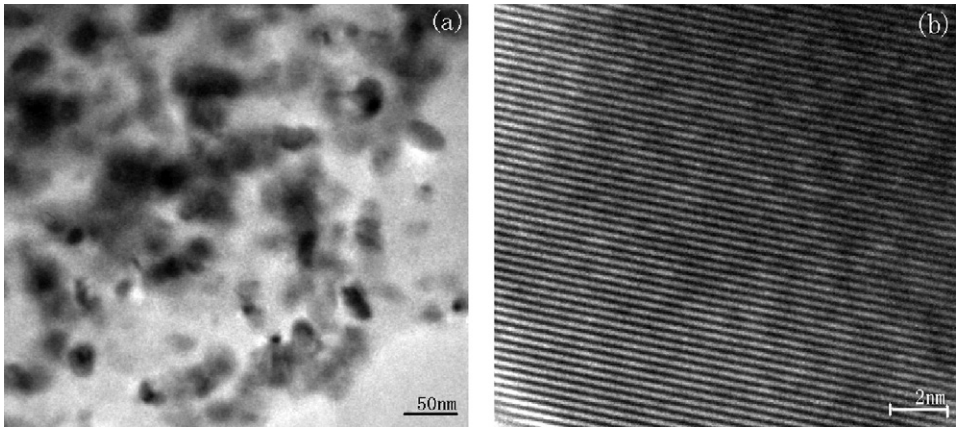

Fig. 2. (a) Low-resolution TEM micrograph of $Zn_{0.92}Fe_{0.08}O$ nanoparticles and (b) high-resolution TEM micrograph of $Zn_{0.92}Fe_{0.08}O$ nanoparticles.

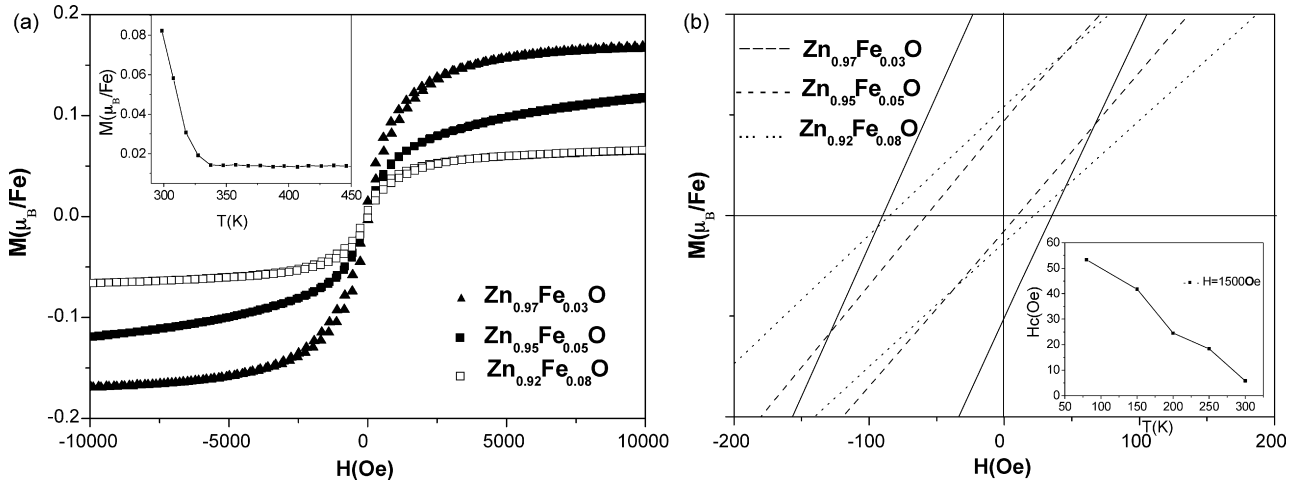

Fig. 3. (a) Magnetic hysteresis (M–H) loops of $Zn_{1-x}Fe_xO$ ($x = 0.03$, 0.05, 0.08) at room temperature under 10 KOe. Inset shows the temperature dependence of magnetic moment for $Zn_{0.92}Fe_{0.08}O$ under 1 KOe and (b) local enlarged patterns for (a) from which clear hysteresis loops can be observed for all samples. Inset shows the temperature dependence of coercive field for $Zn_{0.92}Fe_{0.08}O$ under 1.5 KOe.

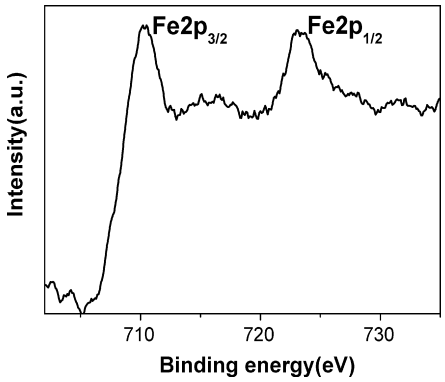

Fig. 4. XPS spectrum of $Zn_{0.92}Fe_{0.08}O$ peak positions are referenced to the adventitious C1s peak taken to be at 284.6 eV.

was Fe_3O_4, the formation of which reduced the value of magnetic moment of the sample [20]. This is another cause of low magnetic moment. In our system, Fe^{3+} ions are present due to the existence of the cation vacancy. A cation vacancy near Fe can promote Fe^{2+} into Fe^{3+} and also mediate the Fe^{2+}–to Fe^{2+} exchange interaction. Since the TM doping percentage is slightly on the higher side toward the cationic percolation threshold, Fe^{2+}–Fe^{3+} exchange, although being less in number in comparison to the Fe^{2+}–Fe^{2+} interaction, may also be possible [15]. And the presence of Fe^{3+} in our samples is a possible signature of hole doping induced by Zn vacancies.

The present theoretical understanding of ferromagnetism in zinc-oxide-based dilute magnetic oxide systems is far from complete. The explanation of our observed ferromagnetism is given by a hybridization picture of super- and double-exchange. The Zn vacancies also play a role for stabilization of the RTFM in $Zn_{1-x}Fe_xO$.

4. Conclusion

In summary, we have prepared Fe-doped ZnO nanocrystals from zinc nitrate and manganese nitrate reduced by citrate with the Fe content up to 10 at.%. The doped limit is around 10 at.% in our experiment settings. The magnetization data show ferromagnetic ordering and exchange bias in $Zn_{1-x}Fe_xO$ ($x \leq 0.08$) at room temperature, The analysis shows room temperature ferromagnetic is an intrinsic property of Fe-doped ZnO, the origin of the ferromagnetic is not due to metallic iron or iron oxides, but given by exchange and Zn vacancies in samples.

Acknowledgements

This work is supported by the National Natural Science Foundation of China (Grant nos. 60778040), gifted youth program of Jilin province (no. 20060123) and the science and technology bureau of Key Program for Ministry of Education (Item no. 207025), the Science and Technology program of "11th five-Year" of Education for Jilin province (no. 2007161 and 2007162).

References

[1] S.A. Wolf, D.D. Awschalom, R.A. Buhrman, J.M. Daughton, S. von Molnar, M.L. Roukes, A.Y. Chtchelkanova, D.M. Treger, Science 294 (2001) 1488.
[2] G.A. Prinz, Science 282 (1998) 1660.
[3] T. Dietl, H. Ohno, F. Matsukura, J. Cibert, D. Ferrand, Science 287 (2000) 1019.
[4] S.J. Pearton, D.P. Norton, K. Ip, Y.W. Heo, T. Steiner, J. Vac. Sci. Technol. B 22 (2004) 932.
[5] X.M. Cheng, C.L. Chien, J. Appl. Phys. 93 (2003) 7876.
[6] K. Ueda, H. Tabata, T. Kawai, Appl. Phys. Lett. 79 (2001) 988.
[7] G.Y. Ahn1, S.-I. Park, S.J. Kim, C.S. Kim, J. Magn. Magn. Mater. 304 (2006) 498.
[8] Y. Lin, D. Jiang, F. Lin, et al., J. Alloys Compd. 436 (2007) 30.
[9] H.-W. Zhang, Z.-R. Wei, Z.-Q. Li, G.-Y. Dong, Mater. Lett. 10 (2007) 1016.
[10] X. Tang, K.-A. Hu, Mater. Sci. Eng. B 139 (2007) 119.
[11] K. Potzger, S. Zhou, H. Reuther, et al., J. Appl. Phys. 88 (2006), 052508.
[12] J.H. Shim, T. Hwang, S. Lee, J.H. Park, S.J. Han, Y.H. Jeong, Appl. Phys. Lett. 86 (2005), 082503.
[13] K. Potzger, S.Q. Zhou, H. Reuther, A. Mücklich, F. Eichhorn, N. Schell, W. Skorupa, M. Helm, J. Fassbender, T. Herrmannsdörfer, T.P. Papageorgiou, Appl. Phys. Lett. 88 (2006), 052508.
[14] Y.Q. Wang, S.L. Yuan, L. Liu, P. Li, X.X. Lan, Z.M. Tian, J.H. He, S.Y. Yin, J. Magn. Magn. Mater. 10 (2007) 1016.
[15] D. Karmakar, S.K. Mandal, R.M. Kadam, P.L. Paulose, A.K. Rajarajan, T.K. Nath, A.K. Das, I. Dasgupta, G.P. Das, Appl. Rev. B. 75 (2007) 144404.
[16] J.H. Yang, L.Y. Zhao, Y.J. Zhang, Y.X. Wang, H.L. Liu, WeiF M.B., Solid State Commun. 143 (2007) 566.
[17] X. Liu, S.Y. Wu, R.K. Singh, N. Newman, J. Appl. Phys. 98 (2005), 046106.
[18] M.S. Seehra, P. Dutta, V. Singh, Y. Zhang, I. Wender, J. Appl. Phys. 101 (2007), 09H107.
[19] A.J. Chen, X.M. Wu, Z.D. Sha, J. Phys. D: Appl. Phys. 39 (2006) 4762.
[20] L. Hedin, J. Phys. C 4 (1971) 2064.